Quantifying the uncertainties in absorption estimates from VSP spectral ratios

Albena Mateeva

ABSTRACT

To make inferences about reservoir conditions such as saturation and permeability from absorption data, one must know how accurate the absorption estimates are. In seismic exploration, absorption is often assessed from VSP spectral ratios, and its uncertainty quantified by the variability of the fitted slope. This greatly underestimates the uncertainty, especially in media with strong scattering. In this paper, I propose ways of quantifying the absorption errors introduced by different factors. Special attention is given to the bias and variability caused by scattering from thin horizontal layers, because it is the largest source of error in stratified media. The next largest uncertainties are associated with receiver positioning and first arrival timing. Ambient noise and event windowing, if properly done, have a much smaller influence on the fitted spectral ratio slopes. When inverting for the quality factor of thick geological units, it may be advantageous to have receiver pairs with a common receiver. However, this introduces a correlation between the spectral ratios, which must be taken into account in the uncertainty analysis of the mean attenuation in the layer. I illustrate the error assessment and absorption estimation steps by a real data example.

1 INTRODUCTION

Absorption carries valuable information about lithology and reservoir conditions, such as saturation and permeability (Winkler & Nur, 1979; Batzle *et al.*, 1996), but to infer them, we must know how accurate the absorption measurements are. In seismic exploration, most absorption estimates come from Vertical Seismic Profiles (VSP). Many people would quantify the reliability of the derived estimates by simply quoting the errors determined when fitting a straight line to the logarithmic spectral ratio between the first arrivals at two depths. At best, this is an optimistic estimate for the uncertainty of the *effective* attenuation caused by both stratigraphic filtering and absorption. The existence of apparent "attenuation" caused by scattering, and particularly by thin layering, is well known (O'Doherty & Anstey, 1971; Schoenberger & Levin, 1974). The quotation marks around attenuation are put because, as I showed previously (Mateeva, 2003), non-stationary reflectivity may cause apparent gain rather than loss of high frequencies through backscattering (reflections from the thin layers immediately beneath a VSP receiver). Using the VSP spectral ratios as an estimator of absorption is acceptable only when the scattering attenuation is small compared to the intrinsic attenuation. Often this is not the case, and the scattering effects must be subtracted from the effective attenuation to get a physically plausible absorption estimate (e.g., a positive Q). In doing so, the bias in the attenuation estimate is removed, but its variability is increased.

Characterizing the bias and variability caused by thin layering is part of the goal of this paper, which is to quantify the total uncertainty in the absorption estimates. Other factors to consider are: uncertainty of the measured traveltime between two VSP receivers, receiver positioning errors when modeling the scattering, spectral distortions due to windowing, and ambient noise. I propose simple ways of quantifying the different uncertainties in the context of a real data example. Eventually, an absorption profile with fair error estimates is obtained.

2 DATA

The data for this study are a VSP with known source and receiving instrumentation signatures, and well-logs acquired in the same borehole. The VSP is used to pro-

file the effective absorption, i.e., the combined action of anelasticity and scattering. Sonic and density logs are used to compute synthetic seismograms from which to assess the share of scattering in the effective attenuation. The known signatures of the VSP source and receiving instrumentation allow us to find the frequency band for most reliable absorption estimation, as well as to evaluate the errors caused by the windowing of first arrivals and ambient noise.

The VSP consists of 175 traces, starting at 150 m below the surface. The depth-coverage is not uniform. The first six receivers are 150 m apart, spanning the the first kilometer of the section. The rest of the receivers are 15 m apart and span the 1-3.5 km interval. The source for the VSP is a vibrator, 70 m away from the borehole head. This offset is negligible compared to the receiver depths. The well-logs start at about 600 m depth and stop at the same depth as the VSP (Fig. 1).

3 MODEL PARAMETRIZATION

Surface seismic images suggest the investigated area is horizontally layered. Thus, we can consider a 1D earth model and invert for the average intrinsic Q of the major geological units. Four main intervals with thicknesses on the order of a kilometer are evident on the well-logs (Fig. 1). It is *a priori* known that there is a thin sandstone layer in the near surface, not captured by the well-logs. I assume that the top interval present in the well logs (600-1000 m) extends up to the base of the thin sandstone layer (the interval appears quite uniform on the VSP data, which start above the well logs). Thus, the preliminary earth model consists of five layers: a thin near-surface sandstone with a quality factor Q_0, and four thick subsurface layers, characterized by mean quality factors Q_1–Q_4. Only the deep layer parameters Q_1–Q_4 can be constrained by VSP spectral ratios because the VSP starts below the sandstone. In principle, Q_0 can be assessed from the signal in the shallowest VSP receiver if the source and receiving instrumentation signatures are known and if the source and receiver coupling with the ground is frequency-independent or known.

Initial estimates of $Q_1 - Q_4$ indicated that the quality factor of the top part of Layer 3 is substantially different from that of its lower part. Indeed, a closer inspection of the well logs reveals a thin layer at about 2500 m depth that may separate the interval into two zones with different fluid contents that result in different Q-values. Thus, I denote them by Q_{3a} and Q_{3b} and assess them separately.

4 METHOD OF ESTIMATING Q

There are a number of approaches to estimating absorption from VSP experiments (Tonn, 1991). The most popular techniques are variations of the spectral-ratio method, developed by Hauge (1981) and Kan (1981). To make this study relevant to as many users as possible, I consider a generic spectral-ratio approach, in which the effective attenuation S_{eff} of a given depth interval $[z_1; z_2]$ is measured by the slope of the log-amplitude spectral ratio between the first arrivals at depths z_1 and z_2,

$$\frac{20}{t_2 - t_1} \log \frac{A(f, z_2)}{A(f, z_1)} = \text{const}_f + S_{\text{eff}}\, f\,, \tag{1}$$

where t_1 and t_2 are the first arrival traveltimes at the respective receivers, and f is frequency. The left hand side of eq. (1) is measurable from VSP data. The slope S_{eff} can be found by a linear regression and is related to the effective quality factor Q_{eff} by $S_{\text{eff}} \approx -27/Q_{\text{eff}}$. In a homogeneously absorbing medium, anelasticity and scattering contribute cumulatively to the effective attenuation, because arrivals with equal traveltimes have suffered the same amount of absorption regardless of their trajectory. Therefore,

$$S_{\text{eff}} = S + S_{\text{sc}} \tag{2}$$

where $S \approx -27/Q$ characterizes the loss of high frequencies caused by absorption (i.e., Q is the intrinsic quality factor) and $S_{\text{sc}} \approx -27/Q_{\text{sc}}$ characterizes the spectral change due to scattering (Q_{sc} is the apparent quality factor). After S_{eff} has been assessed from VSP data (eq. 1), the intrinsic attenuation S, can be isolated by modeling and subtracting the scattering attenuation S_{sc} from S_{eff}. Given a reflection coefficient log, and assuming the medium is horizontally layered, we can compute synthetic seismograms (absorption-free synthetic VSP) from which to get S_{sc} by fitting a line to the spectral ratio between the same two receivers from which S_{eff} was extracted. Note that, while the intrinsic Q is assumed to be frequency-independent, we do not have to assume that Q_{sc} is frequency independent (even though, over the narrow frequency band of the seismic source, it arguably is). By fitting the spectral ratio between synthetic traces by a straight line we do not aim at estimating the total scattering attenuation. We only aim to get its linear component S_{sc} which causes the bias in the effective attenuation (S_{eff} being fit by a linear regression, too).

The intrinsic slope S is always negative (the intrinsic Q is positive). In contrast, the slope S_{sc} can be positive if reflections from below make the signal in the deeper receiver relatively richer of high frequencies than the signal in the shallower receiver (Mateeva, 2003). In other words, contrary to popular belief, scattering does not necessarily lead to an overestimate of the intrinsic absorption. Ignored scattering (thin layering) is the most probable cause for the unphysical, negative Q-factors reported in VSP studies sometimes.

Eq. (2) is strictly valid in homogeneously absorbing media. Of course, in reality, the thin beds responsible for the scattering are likely to have different quality factors. Thus, the medium is not homogeneously ab-

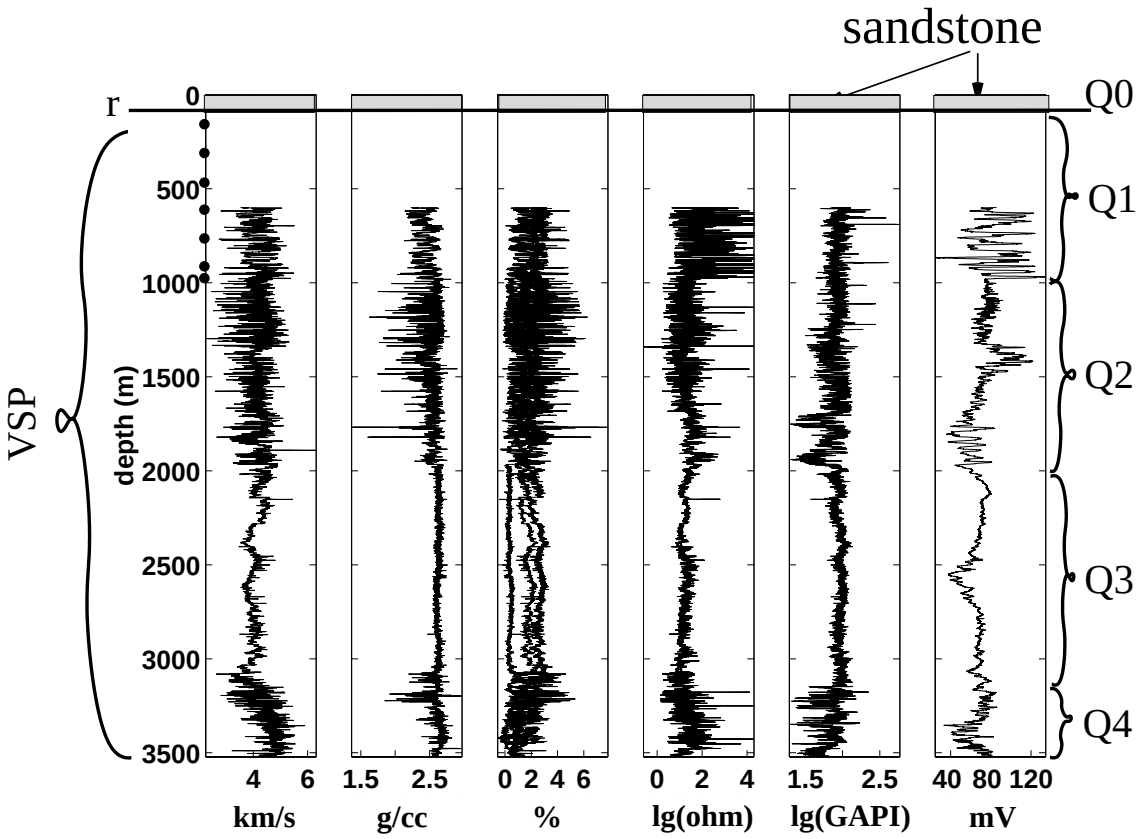

Figure 1. Well-logs used to identify the main subsurface intervals, the mean quality factors $Q_1 - Q_4$ of which are to be determined. Shown on the left is the span of the VSP; dots represent the first 7 VSP receivers (with large non-uniform spacing; the rest of the receivers are close and uniformly spaced). The existence of a sandstone layer in the near surface is known *a priori*; its base with a reflection coefficient r is drawn approximately.

sorbing. However, as long as the absorption is constant on the macro-scale (e.g., withing each thick layer of our model), eq. (2) can still be used, with S being an average characteristic of the region.

5 PREPARATIONS FOR SPECTRAL RATIO ESTIMATION

5.1 Choice of receiver pairs

Suppose a VSP is acquired at n different depths in a given subsurface interval. The n traces can be combined into $n-1$ non-redundant spectral ratios. There are many possible ways to pair the receivers. A reliable absorption estimate is obtained when the slope of the spectral ratio is large compared to its variability. Thus, I chose to maximize receiver separation. In every layer of the model, I paired the receivers from the top half of the layer with the receiver at the bottom of the layer, and the receivers from the bottom half of the layer with the receiver at the top of the layer (Fig. 2a). In this way all traces are used in a non-redundant manner, with minimum receiver separation of about half of the layer thickness.

As a bi-product of the chosen pairing scheme, we get an indication of whether the model discretization is reasonable. For the mean quality factor to be a representative characteristic of a layer, it should not vary too much throughout the layer. One definition of "varying too much" would be the estimated intrinsic Q of the top half of the layer to be substantially different from the intrinsic Q of the lower half. Such instances are easy to spot if we plot a measure of absorption versus receiver separation, as in the cartoon in Fig. 2b. This is how Layer 3 was identified as a candidate for splitting into two sub-layers, as already mentioned in Section 3.

A potential drawback of the proposed scheme for receiver pairing is that anomalies* in the top or bottom receiver would propagate into many spectral ratios and cause systematic errors. Severe problems may be iden-

*An anomaly may be caused by coupling, source variations, noise outbursts, or inadequate scattering simulations (e.g., the source offset not being negligible for a shallow trace).

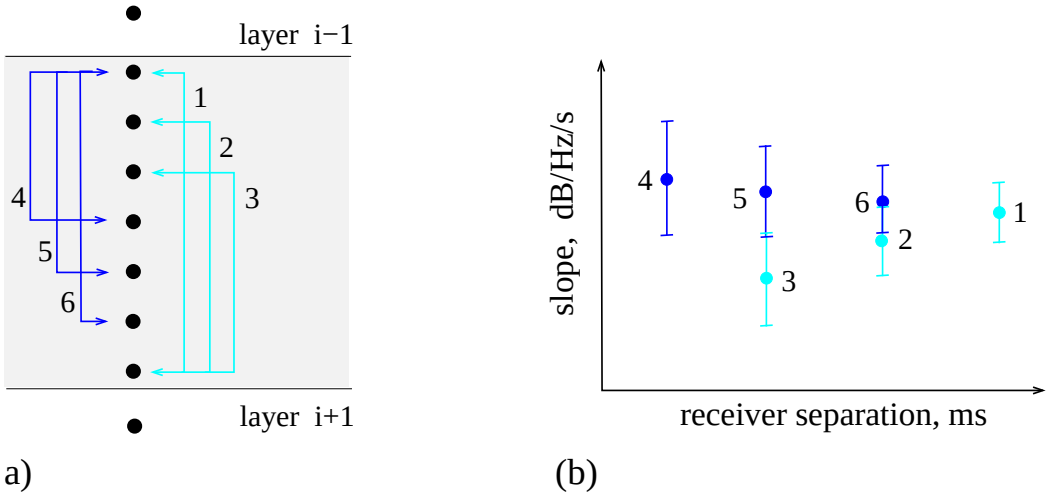

Figure 2. Cartoon: (a) Pairing the receivers in Layer i. Pairs containing the bottom-most receiver will be presented by a light color throughout the paper. Pairs containing the top-most receiver will be presented by a dark color. The distinction is made because the two sets sample different parts of the layer. (b) Indication for significant and systematic absorption variations in Layer i: small-separation pairs that sample predominantly the top or bottom halves of the layer (e.g., 3 and 4) give different estimates of the intrinsic attenuation, while pairs that span most of the layer (e.g., pairs 1, 2 and 6) show similar values for the intrinsic attenuation.

tified in advance by looking at how "typical" the top- or bottom-trace spectra are, but milder abnormalities would be hard to find.

The existence of a correlation between the spectral ratios obtained from receiver pairs with a common receiver must be taken into account when computing the mean attenuation in a layer. Failing to do so would give an erroneous uncertainty estimate for the mean attenuation, even-though the mean attenuation itself would not suffer much because the individual spectral ratios are consistent estimators of it. The covariance matrix needed for fair uncertainty analysis is derived in Appendix A.

5.2 Choice of frequency band

To get meaningful absorption estimates, it is important to identify the frequency band over which the signal to noise ratio is sufficiently high. Since scattering from thin layers will be explicitly taken into account in the absorption estimates, it does not represent "noise" (when not taken into account, this source-generated "noise" is a dominant cause of bias and uncertainty). The noise in our data is the ambient background that can be seen on the VSP traces before the first arrivals. Fig. 3 shows the power spectrum of the noise assessed from windows before the first arrivals together with a model of the signal spectrum, consisting of the known source function (Klauder wavelet), filtered by the known receiving instrumentation responses, and scaled to the first arrival amplitude of a representative VSP trace (a trace in the middle of the profile). As is seen from Fig. 3,

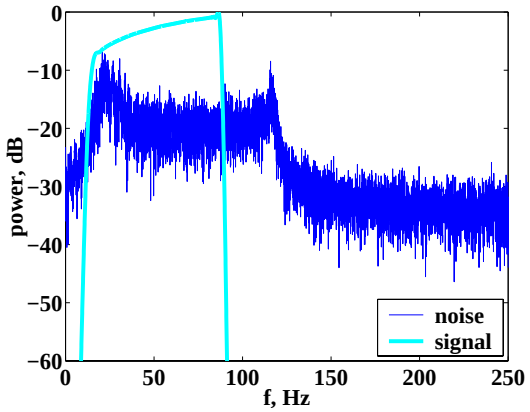

Figure 3. Power spectra of signal (source function filtered through receiver and instrumentation, and scaled to the peak amplitude of a typical VSP trace) and ambient noise.

only frequencies between 15 and 85 Hz can be used for absorption estimation; the rest of the spectrum is dominated by noise. On most traces the signal-to-noise ratio in the usable frequency band is about 20 dB.

6 ERRORS

The main sources of error in the effective and scattering attenuation estimates are discussed below together with strategies for quantifying them.

6.1 Error due to finite time windowing

Spectral-ratios are based on a time window around the first arrival. Suppose $A_2(f)/A_1(f)$ is the true amplitude ratio between the early portions of two traces. What we measure is

$$\frac{W * A_2}{W * A_1} \neq \frac{A_2}{A_1}\,, \tag{3}$$

where $W(f)$ is the amplitude spectrum of the taper (the time window). The taper influence depends on the smoothness of A_1, A_2. A simplistic model of $A_1(f)$ is the signal model in Fig. 3, multiplied by the spectrum of the transmission impulse response of the shallow sandstone[†]. The latter is needed because the reverberations in the sandstone are strong – they roughen the trace spectra (introduce notches). To assess the tapering effects, we can construct "true" spectra $A_2(f)$ by imposing an exponential decay with different Q values on $A_1(f)$, and compare the true slope of A_2/A_1 to the slope fitted to $W * A_2/W * A_1$ for a given taper. Unlike A_2/A_1, the tapered ratio does not fall on a perfect straight line; i.e., tapering not only biases the absorption estimates, it induces some uncertainty in the slope estimates as well. I call the difference between the slope fitted to $W * A_2/W * A_1$ and the true slope the "tapering bias". The residuals of the fit determine the "variability of the bias", which is in fact the variability of the estimated attenuation introduced by the finite time window.

The tapering bias and its variability were measured for a 20% cosine taper with length 64, 128, or 256 samples. Qualitatively, the following was observed (Fig. 4):

- The bias is positive, i.e., negative slopes appear less negative (Q appears higher), while positive slopes corresponding to fictitious negative Q-factors appear even more positive.
- The bias decreases as the true Q increases.
- Longer windows reduce both the bias and the variability of absorption estimates. The bias is reduced because the biases of the individual amplitude spectra in the spectral ratio are reduced. The variability is reduced mainly because of the larger number of frequency samples in the usable frequency band. A longer taper also preserves better the exponential relationship between A_1 and A_2 and allows less leakage of noise from outside the useful frequency band (next section). The increased stability of the spectral ratio slopes estimated from long time-windows has been noted by Goldberg *et al.* (1984) and Ingram *et al.* (1985) when studying spectral ratios between sonic log waveforms.
- For all windows and Q-values tested, the tapering bias was small compared to the other uncertainties in the absorption estimates (quantified later).

Given the latter, I decided to use the shortest 64-sample (128 ms) taper in oder to localize the attenuation estimates as much as possible (a long time window would carry information about regions far away from a receiver pair, especially in a high-velocity medium).

The ordinate values in Fig. 4a and 4b show that the bias and its uncertainty are comparable. Thus, the true slope falls withing the error bars of the measured slope. Moreover, the bias for the 64-point taper is only 1% of the measured slope (compare the vertical to the horizontal scale in the Fig. 4a). Thus, the widowing effect is negligible, despite that the trace spectra are rough. This seems to contradict earlier findings (e.g. Sams & Goldberg, 1990[‡]), and permits us to use relatively simple spectral estimation techniques (e.g. tapering) instead of, say, multi-tapering (Thomson, 1982; Walden, 1990) or data flipping (Pan, 1998). Such more sophisticated methods are needed when attenuation is estimated "point-wise" from individual frequency samples (e.g. Patton, 1988) rather than from the slope fit over many frequencies.

6.2 Ambient Noise

Since background noise is time-windowed together with the signal, it makes sense to consider the combined effect of tapering and ambient noise on the absorption estimates. The bias estimation procedure from the previous section was repeated after adding ambient noise (assessed from windows before the first arrivals) to the time-series corresponding to A_1 and A_2 (Fig. 5). Now the bias is larger than in the noise-free case; namely, it is about 4% of the measured slope for $Q = 5$, 13% of the measured slope for $Q = 50$, etc. (Fig. 5a). As the true Q increases, the absolute value of the bias decreases more slowly than in the noise-free case, and it never goes to zero. This reflects the fact that noise makes the records in two receivers different even if the medium is non-absorbing. Also, unlike in the noise-free case, the true slope is outside the error bars of the measured slope (compare the ordinates in Fig. 5a, 5b).

To quantify the combined effect of background noise and windowing on attenuation estimates, numerical models were derived from the data in Fig. 5. Now both the bias and its variability can be fit by quadratic functions of $\hat{S}$, i.e.,

$$b_S = \alpha_0 + \alpha_1 \hat{S} + \alpha_2 \hat{S}^2 \tag{4}$$

[†]Here the sandstone layer is modeled as a homogeneous slab with one-way time-thickness of 15 ms (Appendix B), bounded by reflection coefficients -1 (top) and -0.45 (bottom).

[‡]A likely explanation is that the notches in our trace spectra occur at the same frequencies at all receivers, and the spectral ratios near them do not fluctuate much more than at other frequencies. This is true even in the presence of noise, when tapering may stabilize the spectra near the notches by "leaking signal" into them from the neighboring regions.

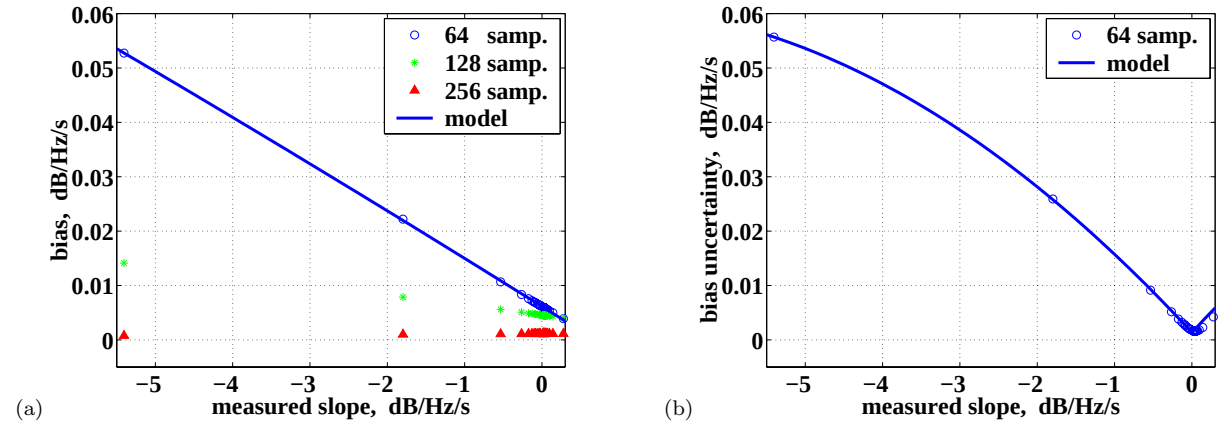

Figure 4. Tapering effects in the absence of noise: (a) slope bias measured over the 15-85 Hz band for three window lengths; the data for the 64-sample window are fit by a linear regression. (b) variability of the bias estimate for a 64-point taper – measured (circles) and fit (solid line) by a quadratic function of the measured slope magnitude.

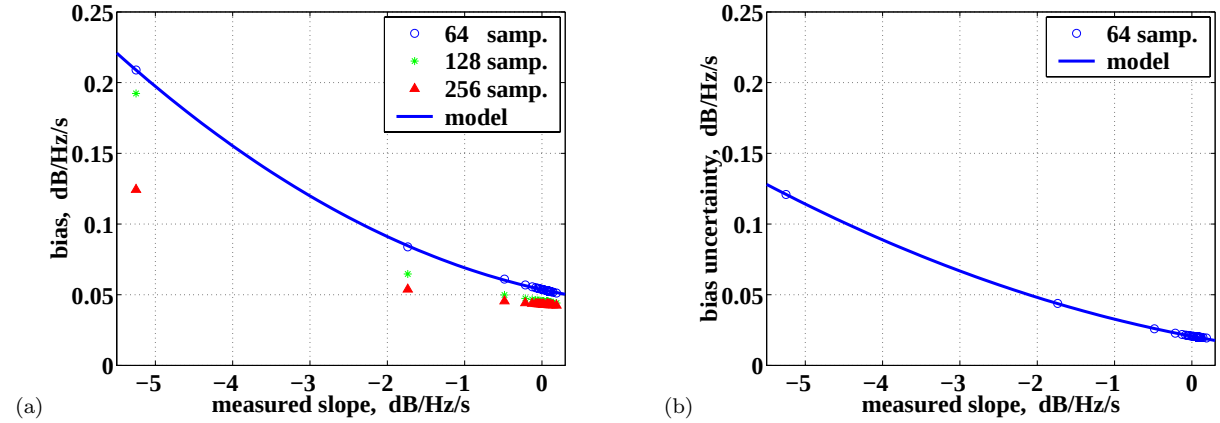

Figure 5. Analogous to Fig. 4 but in the presence of ambient noise: (a) bias for three window lengths; the data for 64-sample taper are fit by a quadratic model. (b) variability of the bias estimate for a 64-point taper – measured (circles) and fit (solid line) quadratic model.

and

$$\mathrm{Var}\,(b_S) = \beta_0 + \beta_1 \hat{S} + \beta_2 \hat{S}^2 \qquad (5)$$

The estimated coefficients $\alpha_{0,1,2}$, $\beta_{0,1,2}$ for the 64-point taper are used later to predict the tapering and ambient noise errors in S_{eff} and S_{sc}.

6.3 Window positioning and traveltime uncertainties

Near the first arrival, seismic traces are not stationary, so the frequency content of an early window is sensitive to its exact position. For spectral ratios to measure the earth filtering, care should be taken to window the same signal on all traces. In the absence of significant dispersion (as in our data set), this can be done by adjusting the window position so that the first arrival peaks at the same instant relative to the beginning of the window on every trace. This is an important detail in the preparation for absorption estimation. Inconsistent windowing causes erratic behavior of the spectral ratios.

The time separation Δt between the receivers in a given pair [$\Delta t = t_2 - t_1$ in eq. (1)] can be measured from the first arrival peaks with a precision on the order of the sampling interval, e.g., $\sigma_{\Delta t} \approx \pm 2$ ms. This uncertainty propagates in the spectral ratio slope as

$$\sigma = \frac{\sigma_{\Delta \mathrm{t}}}{\Delta t}\,\hat{S}\,, \qquad (6)$$

where $\hat{S} = S_{\mathrm{eff}}$, for example.

6.4 Receiver positioning errors in the synthetic seismograms

The timing uncertainty described by eq. (6) is present only in ratios between real VSP traces, not in synthetic

traces (the time separation between them is known). However, since the receiver positions for the synthetic traces are determined by the first arrival traveltimes measured on the VSP traces[§], errors in VSP traveltimes translate into positioning errors in the synthetic data – the receivers in the scattering simulations and those in the real VSP are not identically positioned with respect to the fine structure of the subsurface. As a consequence, the spectra of the synthetic traces do not match wiggle by wiggle the VSP spectra. The *slope* of a spectral ratio is less sensitive to such positioning errors than the spectral ratio itself. That is why I chose to compensate for the scattering effects by first fitting the slopes of the synthetic ratios and then subtracting them from the slopes of the real VSP ratios, rather than first subtracting the synthetic ratios from the VSP ratios and then fitting a slope. The sensitivity of $S_{\rm sc}$ to local interference (that changes with receiver position) depends strongly on the usable frequency band. In our case of a 64-point taper and 2 ms sampling, the usable frequency band has only 11 samples and the slope uncertainty can be significant.

Suppose t is the first arrival traveltime measured on a real VSP trace. Let σ_t denote its uncertainty. This traveltime uncertainty translates into a receiver positioning error in the synthetic VSP, which in turn, leads to a variability σ^2_{pos} in $S_{\rm sc}$. According to the error-propagation method,

$$\sigma^2_{pos} = \left(\frac{d\,S_{\rm sc}}{d\,t}\right)^2 2\,\sigma_t^2 \qquad (7)$$

The coefficient 2 is there because each of the two receivers in the pair from which $S_{\rm sc}$ was estimated has a positioning uncertainty σ_t. For this particular data set I assume $\sigma_t = \pm 1$ ms. The squared derivative in eq. (7) can be assessed by differencing the estimated slopes $S_{\rm sc}$ for each set of receiver pairs with a common receiver (only one receiver is moving), and taking the mean of the squared results, i.e.,

$$\left(\frac{d\,S_{\rm sc}}{d\,t}\right)^2 = \mathop{\rm mean}_i \left(\frac{S_{sc}^{(i)} - S_{sc}^{(i-1)}}{t^{(i)} - t^{(i-1)}}\right)^2 , \qquad (8)$$

where $t^{(i)}$ is the first arrival traveltime at the moving receiver from pair i. I assign the same σ^2_{pos} to all pairs with a common receiver.

6.5 Fitting uncertainties (local interference)

Now let us concentrate on the uncertainties that are inherent to the problem rather than caused by imperfect measurements.

Unlike the intrinsic attenuation which can be described by an exponential law at seismic frequencies, scattering attenuation can be described by a certain law only in a statistical sense. For a given realization of the medium, each frequency is modulated by local interference so that a spectral ratio never falls on a straight line even if the statistical average does. This has several implications to absorption estimation in heterogeneous media:

- A spectral ratio slope estimated from an error-free experiment has a finite uncertainty.
- Effective-attenuation estimates should be corrected for the scattering measured over the *same frequency band* – it can be quite different from that measured over a larger frequency band (Fig. 6). The stronger the scatterers, the larger the deviation of the locally fitted slope from the average can be.
- If $S_{\rm eff}$ and $S_{\rm sc}$ are assessed from the same frequency band, the additional linear trend in $S_{\rm eff}$ caused by the *particular realization* of scattering over the target frequency band is modeled and removed – it is not "noise". Only the residuals of the fit constitute noise in the spectral ratios (both in the real and synthetic VSP). Assuming those residuals are independent and normally[¶] distributed, the uncertainty of a spectral-ratio slope is well known (e.g., Johnson and Wichern, 2002):

$$\sigma_{fit} = \frac{\sigma_e}{\sqrt{n_f}\,\sigma_f}\,, \qquad (9)$$

where σ_e is the standard deviation of the residuals of the least-square fit, n_f is the number of the data points (frequency samples) in the usable frequency band and σ_f is the standard deviation of the frequency samples (i.e., σ_f characterizes the width of the usable frequency band). In a perfect world, the residuals of the fit for a given receiver pair would be the same for the real and the synthetic VSP. In reality, they are only on the same order of magnitude but are not identical mainly because of positioning errors in the synthetic VSP.

7 ESTIMATING ATTENUATION

Now we are ready to derive some attenuation estimates. First, the effective attenuation is evaluated from the VSP data. Then, thin layering contributions are assessed and subtracted to isolate absorption. Finally, the absorption estimates from different receiver pairs are appropriately weighted and averaged to get the mean absorption (mean intrinsic Q) in each layer.

7.1 Effective attenuation from VSP data

The first arrivals on all traces were windowed by a 64-point 20% cosine taper, positioned so that the main

[§]A Goupillaud model is used to generate the synthetic seismograms; thus, receiver "positions" are specified in terms of traveltime from the earth surface.

[¶]In fact, the residual distribution seems sharper than a Gaussian, so eq. (9) may overestimate the slope uncertainty.

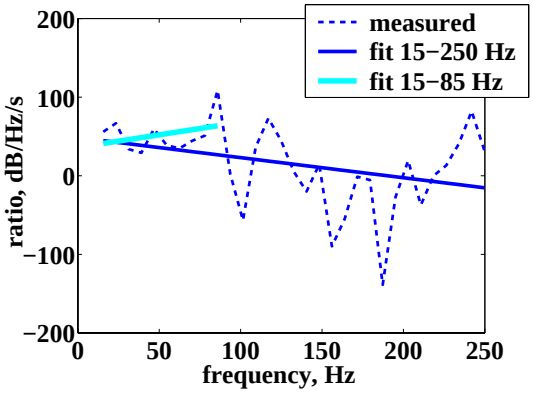

Figure 6. Linear fit in the presence of scattering – the estimated spectral slope depends on the frequency band used.

event was not degraded[‖]. The receivers were paired as illustrated in Fig. 2, and a linear regression was used to fit the spectral ratios on a log-linear scale (eq. 1) over the 15-85 Hz band. The uncertainty of the obtained slope S_{eff} has two main components. One comes from interference [fitting error – eq. (9)], the other comes from measuring the time-separation between the receivers (eq. 6). Thus,

$$\text{Var}\,(S_{\text{eff}}) \;=\; \frac{\sigma_e^2}{n_f\,\sigma_f^2} \;+\; \frac{\sigma_{\Delta t}^2}{\Delta t^2}\,S_{\text{eff}}^2 \qquad (10)$$

Typically, the first term is an order of magnitude larger than the second one.

The error caused by tapering and ambient noise, albeit small compared to the uncertainty (10), is also taken into account. For each receiver pair, the predicted bias (eq. 4) is subtracted from the estimated slope S_{eff} and the slope uncertainty is adjusted according to

$$\text{Var}(S_{\text{eff}} - b_S) = (1 - 2\alpha_1)\text{Var}\,(S_{\text{eff}}) + \text{Var}(b_S), \qquad (11)$$

where $Var(b_S)$ is predicted from S_{eff} by eq. (5), and α_1 is the coefficient from the bias model (eq. 4). This is a very minor adjustment compared to the total uncertainty of S_{eff}.

The so obtained effective slope estimates are shown in the left column of Fig. 7.

7.2 Scattering effects

The synthetic VSP for assessing S_{sc} was computed from the reflection coefficient log in Fig. 8 by a time-domain reflectivity code [*sugoupillaud* from the free software package SU, (Cohen & Stockwell, 2002)], assuming

[‖]Since the first arrival waveform is acausal (distorted Klauder wavelet), the early part of it is inevitably cut by the taper. The "main event" which I tried to preserve starts with the trough before the main peak, and caries most of the energy of the arrival.

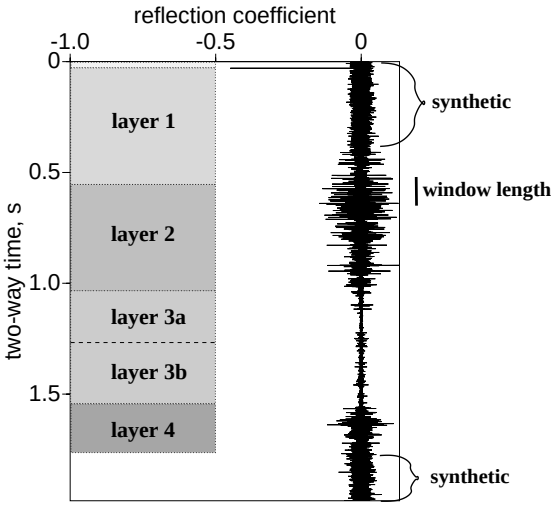

Figure 8. Reflectivity log used to predict scattering effects. Its constrction is described in Appendix B. Shown on the right is the length of the taper used for first arrival windowing.

the medium is horizontally layered and non-absorbing. Spectral ratio slopes were estimated in the same manner as from the real VSP. The only difference is that the slopes S_{sc} contain positioning errors instead of timing errors, i.e., the equivalent of eq. (10) is

$$\text{Var}\,(S_{\text{sc}}) \;\approx\; \frac{\sigma_e^2}{n_f\,\sigma_f^2} \;+\; \sigma_{pos}^2\,, \qquad (12)$$

where σ_{pos}^2 is given by eq. (7). Usually the positioning error σ_{pos}^2 is smaller than the fitting uncertainty (the first term), but larger than the timing error in eq. (10).

The results for S_{sc} are shown in the central column of Fig. 7. Note that these are estimates from the narrow frequency band 15-85 Hz – they quantify the scattering effects as seen by the real VSP, not the scattering effects that would be measured over many realizations of the fine layering or over a larger frequency band. Being strongly influenced by local interference, these values of S_{sc} are hard to predict even qualitatively by looking at the reflectivity log in Fig. 8. For example, S_{sc} tends to be positive in Layer 2, while one would expect it to be negative, given the non-increasing reflection coefficient series in that layer (Mateeva, 2003). Such negative values are readily observable if the spectral ratio slope is fit over a larger frequency band (Fig. 9).

7.3 Intrinsic attenuation (absorption)

Finally, the intrinsic attenuation for each receiver pair is found as $S = S_{\text{eff}} - S_{\text{sc}}$. Its variance is

$$\text{Var}\,(S) = \text{Var}\,(S_{\text{eff}}) \;+\; \text{Var}\,(S_{\text{sc}})\,, \qquad (13)$$

because the effective and scattering attenuation estimators are independent. Since both $Var(S_{\text{eff}})$ and

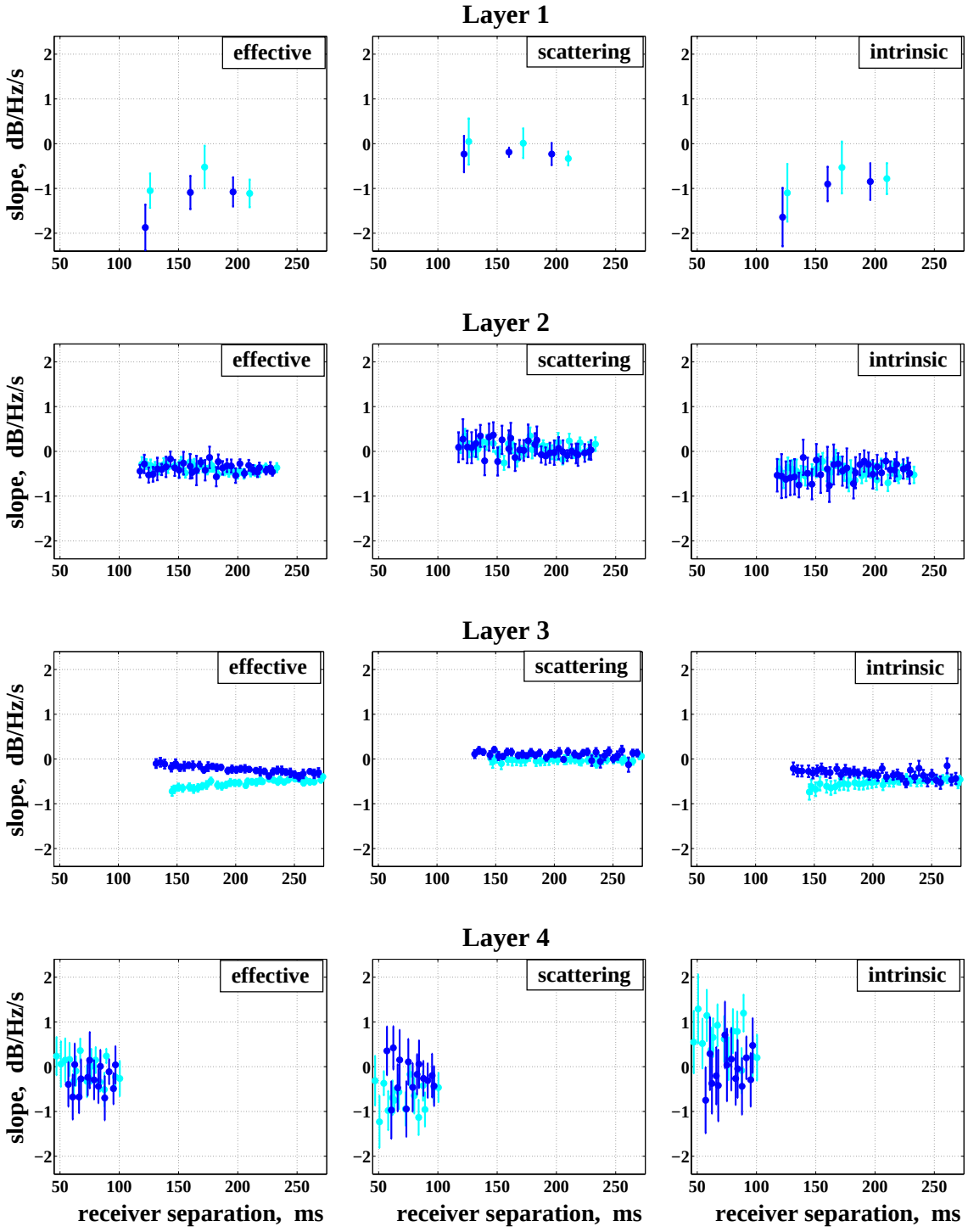

Figure 7. Attenuation estimators: (left) $S_{\rm eff}$ measured from VSP data, (center) $S_{\rm sc}$ measured from synthetic traces in a horizontally layered non-absorbing medium, (right) computed intrinsic attenuation: $S = S_{\rm eff} - S_{\rm sc}$. Dark and light data points correspond to receiver pairs that contain, respectively, the top and bottom receiver in a layer. All plots are on the same scale.

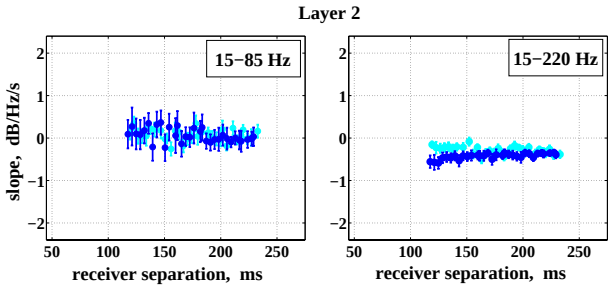

Figure 9. Scattering attenuation estimates in Layer 2 – local fit (left) versus global fit (right). The behavior of the global fit is in an excellent agreement with the theoretical predictions in Mateeva (2002). The local fit is quite erratic.

$Var(S_{\rm sc})$ are dominated by fitting errors (local interference), and the fitting errors are on the same order of magnitude for the VSP and synthetic spectral ratios, the uncertainty of the intrinsic attenuation estimate is about twice as large as that of the effective attenuation (Fig. 7 right).

The results for Layers 3 and 4 call for a comment. The effective attenuation in Layer 3 is clearly larger in the bottom part of the layer than in the top part. The scattering correction has reduced, but not eliminated the trend. This is why I divided the layer in two sub-layers (3a and 3b). The attenuation estimates for these sub-layers are shown in Fig. 10. The intrinsic attenuation in them turns out to be substantially different, indeed.

In Layer 4, a number of receiver pairs (especially among those containing the deepest receiver) give positive $S_{\rm eff}$ and $S_{\rm sc}$; i.e., the signal appears to gain high frequencies with depth. This must be caused by reflections from the fine layering below the deepest receiver and indicates that the reflection coefficient series becomes substantially stronger beneath the borehole (Mateeva, 2003). Unfortunately, this reflectivity change is not observable on the well logs, and thus, is not present in the reflection coefficient log used to predict the scattering effects (Fig. 8). Therefore, scattering and intrinsic attenuation cannot be separated for the deepest VSP receivers which feel the medium beneath the borehole bottom. The intrinsic attenuation can be only assessed from the receivers that feel the "correct" fine layering captured by the well logs. There are ten such receivers in Layer 4, and the attenuation extracted from them is shown in Fig. 11. The reduced receiver separation leads to very large uncertainties. The ten usable receivers give three unphysical, though statistically plausible, intrinsic slopes (Fig. 11 right). I discarded the unphysical slopes when assessing the mean Q of Layer 4.

7.4 Mean intrinsic Q profile

As a last step in obtaining the mean absorption of the subsurface layers, the values of S from different receiver pairs were averaged by a weighted-least-squares procedure within each layer. The covariance matrix for the procedure has diagonal elements σ^2_{ii}, given by eq. (13). The off-diagonal elements σ^2_{ij} are non-zero for pairs i and j that have a common receiver, and are given by (Appendix A)

$$\sigma^2_{ij} \approx \frac{1}{\Delta t_i \Delta t_j} \, \frac{\sigma^2_{A_0}}{n_f \, \sigma^2_{\tilde{f}}} \,, \tag{14}$$

where Δt_i is the time-separation in the i-th receiver pair, and $\sigma^2_{A_0}$ characterizes the uncertainty of the log-amplitude spectrum of the common receiver. It can be estimated by (Appendix A)

$$\sigma^2_{A_0} = \frac{\text{median}\,(\Delta t^2 \sigma^2_e)_{eff}}{2} + \frac{\text{median}\,(\Delta t^2 \sigma^2_e)_{sc}}{2} \tag{15}$$

where the subscripts "eff' and "sc" indicate estimation from the real and synthetic VSP respectively, σ_e is the residuals' standard deviation [as in eqs. (10), (12)], and the median is taken over all pairs sharing the common receiver.

The mean-Q profile ($\bar{Q} = -27/\bar{S}$) resulting from this averaging procedure is shown in Fig. 12. Note that the error bars in Fig. 12 refer to the *mean* quality factor of each layer. They depend both on the variability of the quality factor inside each layer and on the data acquisition and inversion.

Not all estimates in Fig. 12 are the same. Shown by circles are estimates based on all available receiver pairs – they are purely data driven. Such an estimate for Layer 4 (using only 10 receivers) is not feasible because one third of the results correspond to unphysical Q values. I chose to discard them before computing the mean in Layer 4. The result is shown by a different symbol to indicate that this estimate of $\bar{Q}$ is not like the others – it is conditioned by *a priori* knowledge about absorption (i.e., the intrinsic Q is positive). I also computed conditional estimates for Layers 3a and 3b by discarding outliers, even if physically plausible. The results (white crosses) turn out to be compatible with the unconditional estimates, but their error-bars (dashed in white) are smaller. In Layers 1 and 2 there were no obvious outliers.

8 DISCUSSION

The most remarkable feature of the intrinsic Q profile in Fig. 12 is that the absorption of each layer is clearly resolved (outside the error bars of its neighbors), despite that the data set was challenging**. A beneficial factor in obtaining such a result was the dense VSP coverage, providing many data points per layer. Another favorable

**Initial attempts to extract absorption from this particular VSP by feeding it to a commercial flow were unsuccessful.

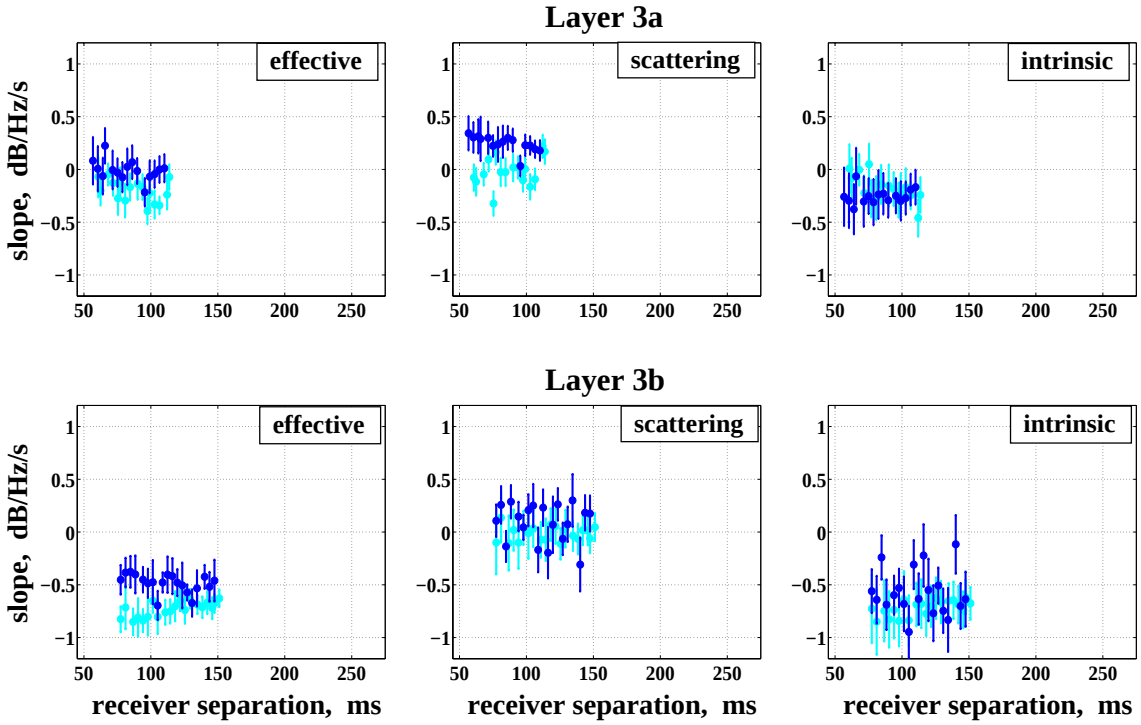

Figure 10. Subdivision of Layer 3 (plots analogous to those in Fig. 7).

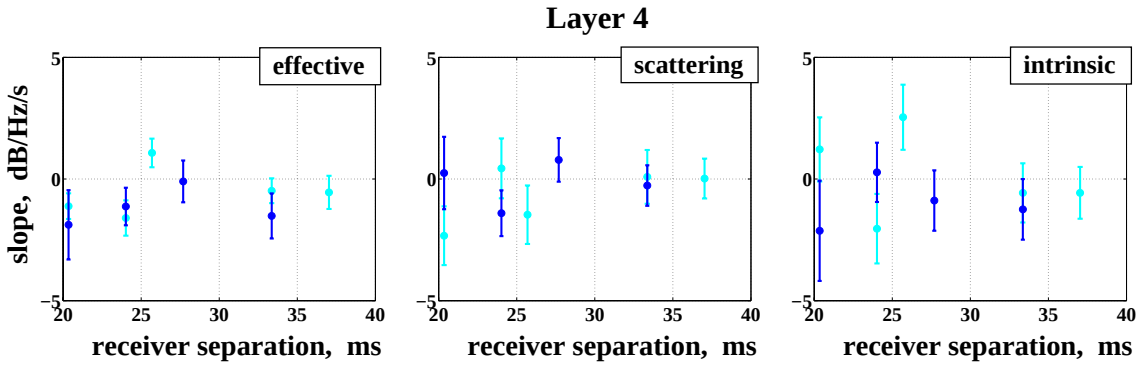

Figure 11. Attenuation estimates in Layer 4 from the top 10 receivers in it, which are not affected by the padding of the reflection coefficient log below the borehole bottom; (plots analogous to those in Fig. 7).

factor is the geology, consisting of thick units with distinct properties and relatively low Q-factors (easier to assess than high Q-s). Last but not least, the reflection coefficient series was not very strong. The correlation between weak scattering and absorption resolution is clearly seen in Fig. 7. Compare, for example, the intrinsic attenuation obtained from pairs with separation 150-200 ms in Layers 3 and 2 (weak and strong reflectivity respectively) – the error bars are larger in the stronger reflectivity. The distinction between the absorption values in the top and bottom halves of Layer 3 would have been impossible in the presence of scattering as strong as that in Layer 2 – the absorption change would have been masked by the large variability of the absorption estimates.

The most uncertain slopes tend to come from pairs with a small separation. Again, this is largely due to scattering effects, rather than timing and positioning errors. If we had a purely transmissional experiment (no reflections from below the receivers), the longer a pulse propagated through the scattering medium, the better the self-averaging in its amplitude spectrum would be. Shapiro and Zien (1993) showed that the standard deviation of the estimated scattering attenuation α is

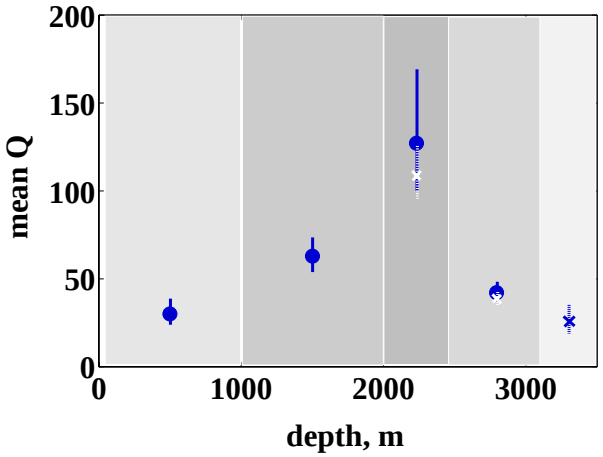

Figure 12. Mean intrinsic Q profile. The background shades visualize the layers, characterized by the mean Q. Circles indicate estimates derived from all available pairs. Crosses indicate conditional estimates, obtained by excluding outliers.

$$\sigma_\alpha \propto \sqrt{\frac{\alpha}{L}}\,, \tag{16}$$

where L is the distance traveled. As $L \to \infty$, σ_α diminishes and the spectral ratio of the output to the input pulse approaches its expected value, e.g., a straight line over a limited frequency band. The inability of the downgoing pulse to stabilize over a short path of propagation, especially in a strong reflectivity, is one of the reasons for the large fitting uncertainties in VSP spectral ratios. An additional reason is that reflections from below cause deviations from linearity in the spectral ratios that do not diminish as the receiver separation increases (they do not self-average). One way to reduce this uncertainty is to fit the spectral ratio over a large frequency band. However, this option is limited by the frequency range of the VSP – we need to assess the scattering as "seen" by the VSP, i.e., over a narrow frequency band. Another way to reduce the uncertainty caused by reflections from below is to separate the up- and down-going wavefields and apply the spectral-ratio method only to the downgoing part (Harris *et al.*, 1992).

To summarize, the uncertainties of all attenuation estimates are larger for pairs with a small separation, and in strong reflectivities. This could have been intuitively expected and has being noted in earlier studies (e.g. Spencer *et al.*, 1982).

It should be pointed out, however, that the scattering in a weak reflectivity can also play an important role in absorption estimation. For example, look at the effective attenuation in the almost homogeneous Layer 3a (Fig. 10, top left). Many of the slope estimates are positive (Q_{eff} is negative). Synthetic seismograms show that is a scattering effect – after correcting for it, the intrinsic attenuation stands at about -0.25 dB/Hz/s (Fig. 10, top right). As an extra benefit from the thin-layering correction, the scatter of the attenuation estimates in Layer 3a has been reduced. This is easily seen for the set of dark data points – compare their alignment before and after the scattering was subtracted. The small scatter of the estimates suggests that, in terms of absorption, Layer 3a is quite homogeneous. The attenuation estimates from different receiver pairs, however, are not always made more consistent by the thin layering corrections – it depends both on the geology and the quality of the estimates. For instance, the scatter of the estimates is increased in Layer 3b, despite that the reflectivity strength in it is comparable to that in Layer 3a. Layer 3b is another illustration of how thin layering effects can be important even when the reflectivity is weak. The *effective* attenuation appears different for the top and bottom parts of Layer 3b (Fig. 10 left). However, the scattering corrections reconcile the results for the two sets of receiver pairs, and the *intrinsic* attenuation does not exhibit a systematic variation with depth (Fig. 10, bottom right).

The price of removing the bias caused by thin layering is increased uncertainty. The variance of S is essentially twice that of S_{eff}. Given the trade-off between bias and variability, is it worthy to correct for the scattering? The conventional way to answer this question is to look at the mean square error (sum of variance and squared bias) of the two absorption estimators. The mean square error (MSE) of the effective attenuation is

$$\text{MSE}\,(S_{\text{eff}}) = \text{Var}\,(S_{\text{eff}}) + S_{\text{sc}}^2\,, \tag{17}$$

while for the unbiased estimator S it is

$$\text{MSE}\,(S) = \text{Var}\,(S) = \text{Var}\,(S_{\text{eff}}) + \text{Var}\,(S_{\text{sc}}) \tag{18}$$

Since in most cases of slope fitting over a narrow frequency band $std\,(S_{\text{sc}}) > |S_{\text{sc}}|$, eqs. (17) and (18) give $MSE\,(S) > MSE\,(S_{\text{eff}})$; i.e., in a mean-square-error sense, the corrected slope S is worse than S_{eff}, at least for an individual receiver pair. For the average attenuation in a layer, it may happen that $MSE\,(\bar{S}) < MSE\,(\bar{S}_{\text{eff}})$ if the scattering compensation makes the estimates of S from different receiver pairs more consistent. In our example, this happens only in Layers 1 and 3a. So it seems that, even in terms of layer averages, the effective attenuation has a smaller MSE than the the intrinsic attenuation.

Unfortunately, this is not a "green light" to ignore the scattering. In some cases it is more important to have an unbiased estimate rather than a small variability. An obvious such case is when S_{eff} is positive (i.e., $Q_{\text{eff}} < 0$). Another case is when the bias due to scattering is large compared to the intrinsic attenuation. Estimates of $|S_{\text{sc}}/S|$ are shown in Table 1. Note that the layer with the highest fraction of scattering (highest albedo) happens to be the almost homogeneous but low-absorbing Layer 3a.

Absorption uncertainties depend on many factors, but, if we are to summarize in coarse figures, we could

	$\lvert S_{\rm sc}/S\rvert$
Layer 1	20%
Layer 2	30%
Layer 3a	70%
Layer 3b	20%
Layer 4	25%

Table 1. Scattering versus intrinsic attenuation – a median estimate over all receiver pairs in a given layer.

say that an absorption estimate derived from a single receiver pair has an uncertainty $\sim 50\%$ (median over all receiver pairs in this study). To reduce it to about 10%, we have to average at least 25 independent estimates. With VSP receiver spacing of $\sim 10^1$ m, that corresponds to a typical absorption resolution of $\sim 10^2$ m.

9 CONCLUSION

To characterize lithology or reservoir conditions from attenuation data, one must separate absorption from scattering effects and have an objective estimate of the absorption uncertainties. The price for removing the scattering is increased variability of the absorption estimates. It is worthwhile to pay if the apparent attenuation is large compared to the intrinsic attenuation. This may happen even when the scattering is weak. Therefore, scattering should not be neglected just because "the medium seems homogeneous" before its share in the effective attenuation has been assessed.

Incoherent scattering is the largest source of uncertainty. A fundamental way to reduce its influence is to have a VSP with a broader frequency band; additional improvement may be sought through wavefield separation. The next largest uncertainties are associated with positioning and timing errors in the synthetic and real VSP respectively. Ambient noise and tapering have a much smaller impact on the fitted slopes. Finally, the correlation between attenuation estimates from pairs with a common receiver must be taken into account when estimating the uncertainty of the mean quality factors of thick geological units.

ACKNOWLEDGMENTS

I thank WesternGeco for supplying the data for this work.

REFERENCES

Batzle, M., Han, D., & Castagna, J. 1996. Seismic Frequency Measurements of Velocity and Attenuation. *Pages 1687–1690 of: SEG Ann. Int. Mtg. Expanded Abstracts*, vol. 66. SEG. RP-1.3.

Cohen, J. K., & Stockwell, Jr. J. W. 2002. *CWP/SU: Seismic Unix Release 36: a free package for seismic research and processing.* Colorado School of Mines.

Goldberg, D., Kan, T. K., & Castagna, J. P. 1984. Attenuation measurements from sonic log waveforms. *Page paper NN of: 25th Ann. Logging Symp.* Soc. Prof. Well Log Analysts.

Harris, P. E., Kerner, C. C., & White, R. E. 1992. Multichannel estimation of frequency-dependent Q from VSP data. *In: EAEG Expanded Abstracts*, vol. 54.

Hauge, P. 1981. Measurements of Attenuation from Vertical Seismic Profiles. *Geophysics*, **46**, 1548–1558.

Ingram, J. D., Morris, C. F., MacKnight, E. E., & Parks, T. W. 1985. Direct phase determination of S-wave velocities from acoustic waveform logs. *Geophysics*, **50**, 1746–1755.

Johnson, R. A., & Wichern, D. W. 2002. *Applied Multivariate Statistical Analysis.* 5 edn. Prentice Hall.

Kan, T. K. 1981. Attenuation Measurements from Vertical Seismic Profiles. *In: SEG Ann. Intern. Mtg. Expanded Abstracts*, vol. 51.

Mateeva, A. A. 2001. Spectral Footprint of Intrabed Multiples. *Pages 255–268 of: CWP Project Review*, vol. 384. Center for Wave Phenomena, Colorado School of Mines.

Mateeva, A. A. 2003. *Distortions in VSP spectral ratios caused by thin horizontal layering.* submitted to Geophys. J. Int., reference No.GD068; also to appear in CWP Project Review Book'2003.

O'Doherty, R. F., & Anstey, N. A. 1971. Reflections on Amplitudes. *Geophys. Pros.*, **19**, 430–458.

Pan, C. 1998. Spectral ringing suppression and optimal windowing for attenuation and Q measurements. *Geophysics*, **63**(2), 632–636.

Patton, S. W. 1988. Robust and least-squares estimation of acoustic attenuation from well-log data. *Geophysics*, **53**(9), 1225–1232.

Sams, M., & Goldberg, D. 1990. The validity of Q estimates from borehole data using spectral ratios. *Geophysics*, **55**(1), 97–101.

Schoenberger, M., & Levin, F. K. 1974. Apparent Attenuation due to Intrabed Multiples. *Geophysics*, **39**, 278–291.

Shapiro, S. A., & Zien, H. 1993. The O'Doherty-Anstey formula and localization of seismic waves. *Geophysics*, **58**(5), 736–740.

Thomson, D. J. 1982. Spectrum estimation and harmonic analysis. *Proc. IEEE*, **70**, 1055–1096.

Tonn, R. 1991. The Determination of the Seismic Quality Factor Q from VSP Data: A comparison of Different Computational Methods. *Geophys. Pros.*, **39**, 1–27.

Walden, A. T. 1990. Improved low-frequency decay estimation using the multitaper spectral analysis method. *Geophys. Prosp.*, **38**, 61–86.

Walden, A. T., & Hosken, J. W. J. 1986. The Nature of Non-Gaussianity of Primary Reflection Coeficients and Its Significance for Deconvolution. *Geophys. Pros.*, **34**, 1038–1066.

Winkler, K., & Nur, A. 1979. Pore Fluid and Seismic Attenuation in Rocks. *Geophys. Res. Letters*, **6**, 1–4.

APPENDIX A: COVARIANCE FOR PAIRS WITH A COMMON RECEIVER

Suppose two spectral ratios, y_1, y_2, are based on a common receiver, i.e.,

$$y_1(f) = \frac{1}{\Delta t_1}\left[P_1(f) - P(f)\right]$$
$$y_2(f) = \frac{1}{\Delta t_2}\left[P_2(f) - P(f)\right] \tag{A1}$$

where P, P_1 and P_2 are log-amplitude spectra, measured at frequencies $f_1, \ldots, f_n$, and $\Delta t_{1,2}$ is the time-separation in the corresponding receiver pair. The covariance between the two spectral ratios caused by the common receiver is

$$\mathrm{Cov}(y_1, y_2) = \frac{1}{\Delta t_1 \Delta t_2}\mathrm{Var}\left[P(f)\right] \tag{A2}$$

Suppose that the amplitude spectra of all traces have equally large uncertainties. Then, as seen from (A1), the variability of the common receiver spectrum can be estimated, for example, by

$$\mathrm{Var}\left[P(f)\right] = \underset{i}{\mathrm{median}}\,\frac{\sigma_{y_i}^2 (\Delta t_i)^2}{2}\,, \tag{A3}$$

where the median is taken over all ratios containing the spectrum $P(f)$, and $\sigma_{y_i}^2$ is the variance of the residuals of the best linear fit of spectral ratio y_i [i.e., $\sigma_{y_i}^2 \approx \mathrm{Var}(y_i)$].

The correlation between the spectral ratios caused by the common receiver propagates in the fitted slopes s_i of $y_i(f)$. As is known from statistical analysis (e.g., Johnson and Wichern, 2002),

$$\mathrm{Cov}\,(s_1, s_2) \approx \frac{\mathrm{Cov}(y_1, y_2)}{n\,\sigma_f^2} \tag{A4}$$

where σ_f characterizes the frequency range over which the spectral ratios were fit. Eq. (A4) is strictly valid for data with Gaussian noise, while the fitting residuals seems to have a distribution that is sharper than a Gaussian, hence the approximate sign.

Substituting (A2) in (A3), and (A3) in (A4), we get

$$\mathrm{Cov}\,(s_1, s_2) \approx \frac{1}{2\,n\,\sigma_f^2}\frac{\mathrm{median}\left(\sigma_{y_i}^2\,(\Delta t_i)^2\right)}{\Delta t_1 \Delta t_2} \tag{A5}$$

This equation is applied separately to the real and synthetic VSP-s to get the off-diagonal elements of the covariance matrix needed when averaging slopes within a macro-layer.

APPENDIX B: REFLECTIVITY LOG FOR MODELING THE SCATTERING EFFECTS

To compute synthetic seismograms, a Goupillaud model was used, i.e, an earth model, consisting of horizontal layers of equal time thickness. The reflection coefficient (RC) series defining such a model is computed from sonic and density logs. After converting it to the time domain and interpolating to the nearest uniform time-grid, one may anti-alias filter and resample to the VSP rate (e.g., 2 ms t.w.t.). I did not resample because the computation of the synthetic seismograms from the full reflectivity log was fast enough; later, I used only the low-frequency part of the synthetic spectra to evaluate scattering.

The well logs span only the 600-3500 m interval. To fill in the missing reflectivity of the upper 600 m, I assumed that the top sequence present in the reflectivity log (600-1000 m) extends up to the surface. I combined its amplitude spectrum with a random phase spectrum, drawn from a uniform distribution $U[-\pi, \pi]$, and inverse-Fourier transformed to the time domain to create a synthetic RC with which to append the real log. The magnitudes of the synthetic reflection coefficients do not follow a mixed Laplace distribution as the real ones do (Walden & Hosken, 1986). However, this does not matter in the apparent attenuation estimation which, in my experience, depends mainly on the power spectrum of the RC series.

In the same manner the reflectivity log was extended below the borehole bottom using the power spectrum of the reflection coefficient log in Layer 4 (3100-3500 m). This was needed because the deepest VSP receivers feel the medium below the borehole; to predict the scattering effects in them, we need a model of the reflectivity below the borehole.

Finally, the near-surface sandstone layer was added by putting a reflection coefficient of -0.45 at 15 ms o.w.t. below the earth surface. The time thickness of the sandstone was determined from notches in the spectra of the VSP traces. The choice of the reflection coefficient magnitude was a bit arbitrary. The main consideration was that it should be large compared to the other coefficients in order to create such strong notches. An additional requirement was that it be consistent with the VSP and well-log data. Continuing the sonic log trend up to the sandstone base suggests a sub-sandstone velocity of roughly 3400 m/s. Then, a reflection coefficient of -0.45 can be explained by a 20 m thick sandstone with a velocity 1300 m/s, which is a plausible model. Tests with slightly different values led to virtually identical estimates of S_{sc}. Similarly, the synthetic spectral ratios are not sensitive to the earth's surface reflection coefficient. For a free surface, it is appropriately set to -1 (as "seen" from above by the displacement field). However, given that the thin sandstone layer is expected to have a very low quality factor, it may be more appropriate to model the earth as bounded by a semi-absorbing surface with a smaller reflection coefficient. In general, it is very important to account for the earth's surface in apparent attenuation studies (Mateeva, 2001). However, the spectral ratios between *early* windows on VSP traces are an exception in that they are not sensitive to the properties of the near surface (Mateeva, 2003).